2011

# Fe-Fe adatom interaction and growth morphology on graphene

Xiaojie Liu
*Iowa State University*

Cai-Zhuang Wang
*Iowa State University*, wangcz@ameslab.gov

Myron Hupalo
*Iowa State University*, hupalo@ameslab.gov

Wen-Cai Lu
*Jilin University*

Patricia A. Thiel
*Iowa State University*, thiel@ameslab.gov

*See next page for additional authors*

# Fe-Fe adatom interaction and growth morphology on graphene

**Abstract**
The nucleation and growth of Fe on graphene is highly unusual. A constantly increasing island density indicates the presence of strong, predominantly repulsive, adatom interactions. We study these interactions by first-principles calculations to identify their origin. We find that the interactions consist of a short-range attraction and longer-range repulsion. We show that electric dipole-dipole interaction can contribute only part of the repulsive force (~30%) between Fe adatoms, and the repulsion due to the elastic interaction is small. We suggest that the dominant contribution to the repulsive energy would originate from the indirect (or RKKY) interactions mediated through the delocalized electrons on graphene.

**Keywords**
Ames Laboratory, Materials Science and Engineering, Physics and Astronomy

**Disciplines**
Chemistry | Materials Science and Engineering | Physics

**Comments**
This article is from *Physical Review B* 84, no. 23 (2011): 235446, doi:10.1103/PhysRevB.84.235446.

**Authors**
Xiaojie Liu, Cai-Zhuang Wang, Myron Hupalo, Wen-Cai Lu, Patricia A. Thiel, Kai-Ming Ho, and Michael C. Tringides

# Fe-Fe adatom interaction and growth morphology on graphene

Xiaojie Liu,[1,2] C. Z. Wang,[2,*] M. Hupalo,[2] Wen-Cai Lu,[1,3,†] P. A. Thiel,[4] K. M. Ho,[2] and M. C. Tringides[2]

[1]*State Key Laboratory of Theoretical and Computational Chemistry, Institute of Theoretical Chemistry, Jilin University, Changchun, Jilin 130021, P.R. China*

[2]*Ames Laboratory–US Department of Energy, and Department of Physics and Astronomy, Iowa State University, Ames, Iowa 50010, USA*

[3]*College of Physics and Laboratory of Fiber Materials and Modern Textile, the Growing Base for State Key Laboratory, Qingdao University, Qingdao, Shandong 266071, P.R. China*

[4]*Ames Laboratory–US Department of Energy, Department of Chemistry and Department of Materials Science and Engineering, Iowa State University, Ames, Iowa 50011, USA*

(Received 6 December 2011; published 27 December 2011)

The nucleation and growth of Fe on graphene is highly unusual. A constantly increasing island density indicates the presence of strong, predominantly repulsive, adatom interactions. We study these interactions by first-principles calculations to identify their origin. We find that the interactions consist of a short-range attraction and longer-range repulsion. We show that electric dipole-dipole interaction can contribute only part of the repulsive force (∼30%) between Fe adatoms, and the repulsion due to the elastic interaction is small. We suggest that the dominant contribution to the repulsive energy would originate from the indirect (or RKKY) interactions mediated through the delocalized electrons on graphene.

DOI: 10.1103/PhysRevB.84.235446 PACS number(s): 68.43.Bc, 68.37.Ef, 68.65.Pq, 73.22.Pr

## I. INTRODUCTION

Recently, adsorption of metal adatoms and growth of metal nanostructures and thin films on graphene have attracted a lot of interests. It has been demonstrated that the electronic and magnetic properties of graphene can be manipulated by metal atom adsorption or doping.[1–8] Metal nanostructures and thin films on graphene can also serve as desirable systems for spintronics and supported catalysis applications.[5–8] Moreover, the study of metal adsorption on graphene is important for a better understanding of the quality of metal contacts, which is very critical to the performance of graphene-based microelectronics devices.

Using scanning-tunneling microcopy (STM) and first-principles calculations, we have shown that different metals on graphene exhibit very different growth morphologies that can be related to the ratio of the adatom adsorption energy on graphene to the bulk cohesive energy of the metals, as well as the diffusion barriers of the metal adatoms on graphene.[5–8] However, many intriguing features in the growth morphologies still cannot be explained simply by the adsorption energy and diffusion barrier of single adatom. In particular, the possibility for strong metal adatom-adatom interactions mediated through graphene and the effects of such interactions on metal nanostructure formation deserve further investigation.

In a recent paper,[9] the interaction of potassium adatoms on graphite has been studied by STM experiments and molecular dynamics simulations. It was proposed that the interaction between K adatoms is mainly due to long-range electric dipole-dipole interactions because of a significant charge transfer from K adatoms to graphite. Despite the high value (∼10 Debye (D)) of the dipole moment, it has no effect on the diffusion barrier. In this paper, we will show that the nature of the interaction for Fe-Fe adatom interaction on graphene is very different from that of K adatoms on graphite and has a strong effect on the diffusion barrier that is responsible for the strong dependence of the nucleated island density on coverage. Although electric dipole-dipole interactions can contribute partially to the repulsive force between Fe adatoms on graphene, our calculation and analysis suggest that the dominant contribution would originate from the indirect (or RKKY) interaction mediated through the delocalized electrons on graphene.

## II. EXPERIMENTAL STUDIES

STM experiments were carried out to study the epitaxial growth of Fe on graphene prepared by thermal annealing of SiC. The method produces G1(single layer) or G2 (bilayer) graphene of very high quality with domains that extend over micrometers because of a slow and controlled desorption of Si through the steps to a graphitized surface.[10] The steps undergo a single- to triple-step transition with different retracting speeds that results in fine coverage control of the remaining C that eventually produces uniform graphene layers over very long distances.

For a different type of graphene (i.e., graphene grown on transition metal substrates), the interaction between the graphene and the substrate distorts the graphene.[11] This controls the growth morphology of the metal islands on graphene because the nucleation sites are regular and defined by the Moire pattern formed by the graphene and substrate lattices.[11] However, in our present experiment the interaction between graphene and Si-terminated SiC substrate is much weaker.[12] As we have shown in previous publications,[5–8] the growth morphology of metal islands on graphene with a Si-terminated SiC substrate is dominated by the interaction between the metal adatoms and graphene. Different metal on graphene/SiC exhibits very different growth morphologies depending on their interaction with graphene (weak vs strong).

Figure 1(a) shows an area of $150 \times 150$ nm$^2$ with 1.05 ML of Fe deposited at 450 K with a flux rate $5.33 \times 10^{-2}$ ML/min. The nucleated island density deviates from standard nucleation behavior at least in two aspects. All the observed islands are three dimensional (3D), with average heights ranging from

 

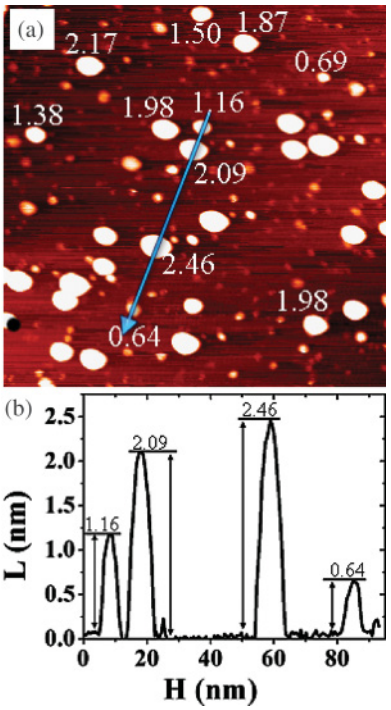


FIG. 1. (Color online) (a) 150 × 150 nm$^2$ STM image for $\theta$ = 1.05 ML of Fe deposited on graphene at $T$ = 450K with a flux rate of 5.33 × $10^{-2}$ ML/min. Taller, brighter islands grow up to a maximum lateral size; smaller ones of suppressed color nucleate at later time. The average heights of small-sized islands is one layer, six layers for medium-sized islands, and 12 layers for large-sized islands. (b) One-dimensional profile through the islands showing typical height distribution.

one layer for small-sized islands, six layers for medium-sized islands, and 12 layers for large-sized islands. Line scans along small, medium, and large Fe islands are also shown in Fig. 1(b). The islands grow even higher with increasing Fe deposition because of the higher cohesive to adsorption energy ratio.[7] The second deviation from standard nucleation behavior is more important and unique to Fe. According to the scaling theory of nucleation,[13] after a maximum island density $n$ is reached and the island separation becomes comparable to the diffusion length, $n$ should remain constant. Steady state is maintained (before island coalescence), with all the newly deposited atoms reaching the islands already on the surface before encountering another monomer to form a new island. This is observed in practically all previous nucleation studies and for other metals deposited on graphene.[5–8] Fe island nucleation on graphene is an exception. Even if all the islands were 3D, as with the same ∼12 layers shown in Fig. 1, depositing 0.5 ML is more than sufficient for steady state to be attained and for $n$ to reach its saturated value according to traditional nucleation theory. However, steady state is not attained, and islands continue to nucleate with deposited amount $\theta$ for Fe on graphene. This is clearly visible from the islands in Fig. 1. New islands nucleate very close to large or medium-sized islands at a distance of less than 5 nm, as shown in Fig. 1(a). The island density observed in Fig. 1 is 6.7 × $10^{-3}$ islands/nm$^2$ (which is one of the highest densities of magnetic islands at such high temperature), and with further deposition to 3.3 ML, it can reach 1.5 × $10^{-2}$ islands/nm$^2$.

## III. FIRST-PRINCIPLES CALCULATIONS

To gain insight into the unusual Fe growth morphology observed in the STM experiments, we have performed first-principles calculations to study the interaction between Fe adatoms on graphene. The first-principles calculations are performed using the density functional theory (DFT) with generalized gradient approximation (GGA) in the form of PBE[14] implemented in the VASP code,[15,16] including spin polarization and dipole moment corrections.[17,18] Valence electrons are treated explicitly, and their interactions with ionic cores are described by projector-augmented wave pseudopotentials.[19,20] The adatoms/graphene system is modeled by having two adatoms at different separations on a 7 × 7 graphene supercell with periodic boundary conditions. The dimension of the supercell in the $z$ direction is 15 Å, which allows a vacuum region of about 12 Å to separate the atoms and their replicas in the $z$ direction. The wave functions are expanded in a plane wave basis set with an energy cutoff of 600 eV. A $k$-point sampling of 3 × 3 × 1 Monkhorst–Pack grids in the first Brillouin zone and a Gaussian smearing with a width of $\sigma$ = 0.05 eV are used in the calculations. All atoms in the supercell are allowed to relax until the forces on each atom are smaller than 0.01 eV/Å. The supercell dimensions are kept fixed during relaxation. Because of interactions between graphene and the Si-terminated SiC substrate are very weak, a free-standing graphene model is a good approximation for *ab initio* calculation studies of metal adatom adsorption and interaction.

The interaction energy between the two adatoms on graphene is defined as $E_{\text{inter}}(r) = E_{\text{a2}}(r) - 2E_{\text{a1}}$. Here, $E_{\text{a2}}(r)$ is the adsorption energy of two Fe adatoms on graphene at separation $r$, and $E_{\text{a1}}$ is the adsorption energy of a single Fe adatom. Figure 2 shows $E_{\text{inter}}(r)$ as a function of $r$ between the two adatoms. It is interesting to note that the interaction between Fe-Fe adatoms is attractive at small separations (less than about 4.0 Å) but becomes repulsive at larger distances greater than 5.0 Å. Because of the finite supercell size used,

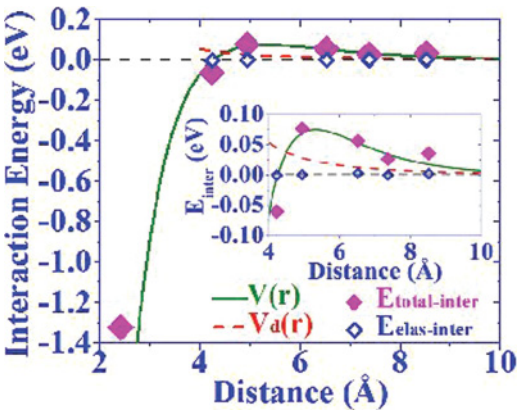


FIG. 2. (Color online) Interaction energy $V(r)$ (solid diamonds and green solid line) of Fe-Fe adatoms on graphene as a function of Fe-Fe separation. $E_{\text{elas-inter}}$ (open diamonds) and $V_{\text{d}}(r)$ (red dash line) are elastic interaction and dipole-dipole interaction, respectively.

the interaction energy from the first-principles calculations may also contain the interaction of the adatoms with their replicas due to the periodic boundary conditions. To correct these artificial interactions, we model the interaction potential as $V(r) = D_e(2e^{-\beta(r-r_e)} - e^{-2\beta(r-r_e)})$ where the parameter $D_e$ can be interpreted as the barrier of the repulsive interaction and $r_e$ is the location of the barrier. The three parameters in $V(r)$ are then determined by fitting the interaction energy as a function of adatom separation from the first-principles calculations, including the interaction with all replicas up to a large cutoff distance of 50 Å. Further increasing the cutoff distance does not alter the fitting parameters. The potential parameters from such a fitting procedure are $D_e = 0.751$ eV, $r_e = 0.532$ Å, and $\beta = 6.54$ Å$^{-1}$. This interaction potential is also shown in Fig. 2 (solid green line). It clearly shows that the Fe adatoms exhibit a strong attraction at small distance, which becomes repulsive when separation of the Fe adatoms is larger than 5.0 Å.

The repulsive interactions for Fe adatoms at large distances can account for the unusual nucleation of Fe islands on graphene. The diffusion length of Fe adatoms at lower coverage (~0.003 ML) and at a temperature of 450 K estimated from the experimentally observed island density based on the scaling theory of nucleation[13] would be at least 50 times larger than 5 nm, where newly formed islands are seen to nucleate [see Fig. 1(a)]. If the only controlling barriers are terrace diffusion and aggregation to the islands, there is no reason for the diffusing adatom not to join the islands. So apparently, there is a barrier that prohibits adatoms from approaching the islands already presented, and the adatoms continue to diffuse on the vacant part of the surface, even very close to the preexisting islands. Encountering another adatom that was also repelled from preexisting islands results in ongoing nucleation of new islands. The origin of this repulsive barrier is related to the Fe-Fe repulsive interactions calculated above.

We have also examined the electronic structure of the adatoms/graphene system in more detail to understand the origin of crossover from an attractive to a repulsive interaction between Fe adatoms. We have calculated the bonding charge distribution (BCD) $\Delta\rho(r)$ which is defined as $\Delta\rho(r) = \rho(r) - [\rho_{gra}(r) + \rho_{ads}(r)]$ where $\rho(r)$ is the charge density of the Fe-Fe/graphene system, $\rho_{gra}(r)$ and $\rho_{ads}(r)$ are the charge densities of pure graphene, and the pair of Fe adatoms calculated separately. The $\Delta\rho(r)$ defined in this way accounts for the charge redistribution due to the interaction between Fe-Fe and graphene. To see the electronic interactions between two adatoms clearly, the 2D-contour of $\Delta\rho(r)$ in the plane normal to the surface and through the two Fe adatoms are plotted in Fig. 3. We can see that when the distance between the two Fe adatoms is smaller (e.g., $r = 2.40$ Å), the induced charge on the two Fe adatoms strongly overlaps, resulting in a strong attractive interaction between the two adatoms. As the distance between the two Fe adatoms increases, the induced charge is well separated and localized on each adatom. It is interesting to note that the charge distribution between the adatoms not only affects their interaction but also alters their electric dipole moment and magnetic moments dramatically. As shown in Fig. 4, at the distance of 2.40 Å where the interaction between the Fe adatoms is strongly attractive, there is a negligible electric dipole moment and a larger magnetic

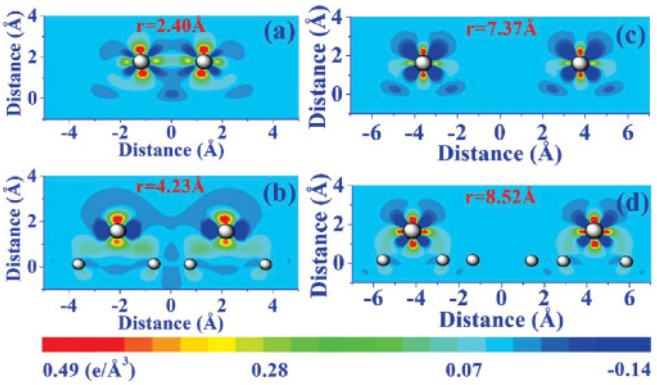


FIG. 3. (Color online) Two-dimensional contours of the bonding charge distribution in the plane normal to the surface and through two Fe adatoms on graphene.

moment of 3.2 $\mu_B$. The dipole moments then increase rapidly to a value of 1.91 Debye as the distance between the two adatoms increases; at the same time, the magnetic moments drop to 2 $\mu_B$.

Whereas the strong attractive interaction between the Fe adatoms at small separation is due to metallization effects, the origin of the repulsive interaction at larger distances is more complex. One source of repulsion is due to electric dipole-dipole interaction, as reported for K adatoms on graphite.[9] Electric dipole-dipole interaction for two non-overlapping dipoles perpendicular to the graphene layer and at a distance $r$ is $V_d(r) = \frac{\alpha}{4\pi\varepsilon_0}\frac{\mu_1\mu_2}{r^3}$. Here $\mu_1$ and $\mu_2$ are the electric dipole moments on each Fe adatom, respectively. The $\alpha$ value should be 1.0 if the two dipoles are in a vacuum and 2.0 if on a metal surface due to the screening effect.[21] Since graphene is a 2D system and the density of free carrier is expected to be smaller than that on a metal surface, the screening effects should be weaker than that on a metal surface, and the $\alpha$ value should be between 1.0 and 2.0. Using the electric dipole moments, as shown in Fig. 4, and $\alpha = 1.5$, the dipole-dipole repulsive energy $V_d(r)$ as the function of distance $r$ is also plotted in Fig. 2 (red dashed line). $V_d(r)$ accounts for only about one third of the total interaction energy, as seen in Fig. 2. Therefore, electric dipole-dipole interaction can partially contribute to the repulsive interaction in this system, but it is not the dominant one.

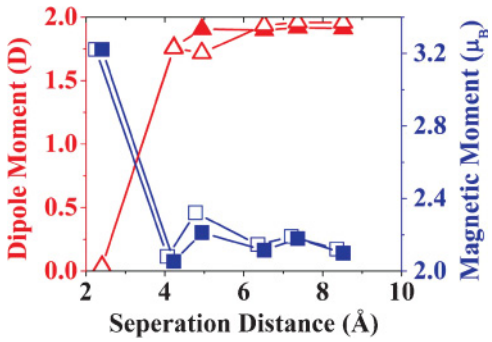


FIG. 4. (Color online) Induced electric dipole and magnetic moment on each Fe adatom with (solid symbols) or without (open symbols) graphene distortions as a function of Fe-Fe separation.

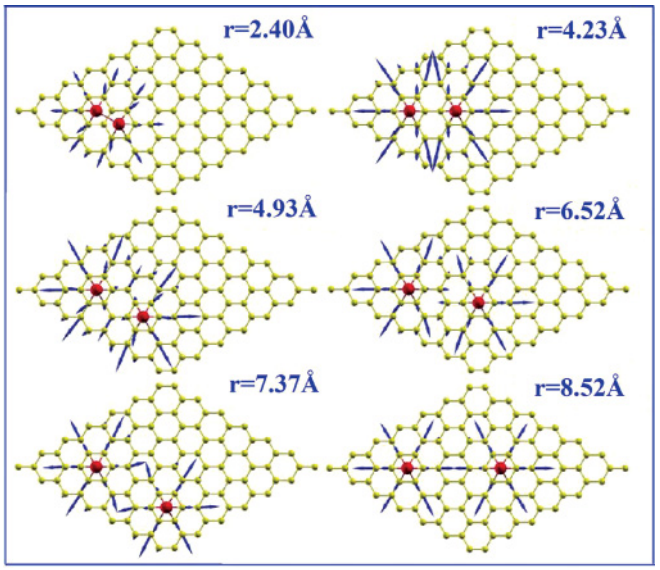


FIG. 5. (Color online) In-plane lattice distortion in the graphene induced by Fe adatom adsorption. The displacements shown by the arrows are enlarged by a factor of 5000 for a clear visualization.

We note that one distinct feature that makes Fe adatoms different from alkali and other simple metals on graphene is that they induce significant lattice distortions. The repulsive interaction between the Fe adatoms would also originate from elastic interactions due to these lattice distortions. Figure 5 shows the in-plane distortion patterns in graphene induced by the two Fe adatoms at different distances. To visualize clearly the distortions, the displacements indicated by the blue arrows in the plots have been enlarged by a factor of 5000. More quantitative analysis of the lattice distortions is shown in Fig. 6, where the amplitude and the square root of the mean square lattice displacements (RMSDs) as a function of Fe-Fe separation are plotted. It is interesting to note that the lattice displacements increase initially, reach a maximum between 4 and 5 Å, then decrease with Fe-Fe separation. This trend of lattice distortion exhibits some correlation with the behavior of interaction energy shown in Fig. 2, suggesting that the elastic interaction may also play a role in determining the interaction energy between the two Fe adatoms.

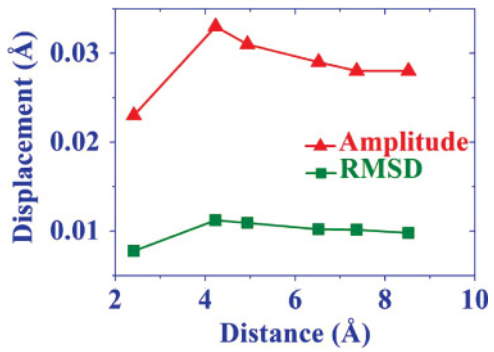


FIG. 6. (Color online) In-plane distortion amplitude and the root mean square lattice displacements (RMSDs) as a function of Fe-Fe separation.

To get an estimation for the magnitude of the elastic interaction between the two adatoms, we repeat the first-principles calculations for the total interaction energy between the two Fe adatoms as described above, with the graphene lattice fixed at its undistorted position (i.e., $E^0_{\text{inter}}(r) = E^0_{\text{a2}}(r) - 2E^0_{\text{a1}}$, where $E^0_{\text{a2}}(r)$ is the adsorption energy of two Fe adatoms at separation $r$ on undistorted graphene and $E_{\text{a1}}$ is the adsorption energy of a single Fe adatom on undistorted graphene). We find that the electronic properties (e.g, electric dipole and magnetic moments) from the fixed and unfixed lattice calculations are very similar, as one can see from Fig. 4. This result suggests that the difference between the total interaction energies from the distorted and undistorted calculations is a reasonable measure of the elastic interaction energy between the two adatoms due to the adsorption-induced graphene lattice distortion. The elastic interaction energy obtained in this way is plotted in Fig. 2. To our surprise, the elastic interaction is very small; even adatom adsorption can induce as large as 2.5% of graphene lattice distortion relative to that of the C-C bond length in graphene.

Another possible source of the long-range repulsion would come from the indirect (or Ruderman–Kittel–Kasuya–Yosida [RKKY]) interaction mediated through the delocalized electrons on graphene due to Friedel oscillation.[22–27] However, quantitative evaluation of the RKKY interaction between the two Fe adatoms mediated through the graphene layer is not a trivial task and is beyond the capability of the present DFT calculations. Nevertheless, since the sum of the electric dipole-dipole interaction and elastic interaction discussed above account only for a small fraction of the total interaction energy, we can conclude that the main contribution of the repulsive interaction between the two Fe adatoms likely originates from the indirect (or RKKY) interaction mediated through the delocalized electrons on graphene.

## IV. CONCLUSIONS

An unusual type of nucleation has been observed for growth of Fe on graphene that is different from classical nucleation. Surprisingly the nucleated density does not reach saturation. A coverage-dependent diffusion length that decreases with increasing coverage must hold: as more atoms are deposited, repulsive interactions prohibit the adatoms from reaching preexisting islands and instead nucleate new islands. This is confirmed from first-principles calculations that show indeed the Fe-Fe interaction between two Fe adatoms has a strong long-range repulsive component that should reduce adatom aggregation to islands. This interaction should be amplified when the diffusing atom approaches a preexisting island with several Fe adatoms exerting repulsion. The current work illustrates how adatom interactions can modify the nucleation process but, more importantly, shows the formation of a controllable high density of magnetic islands that can be of interest in computer storage applications.

## ACKNOWLEDGMENTS

We are grateful to Jim Evans and Dajiang Liu for useful discussions. Work at Ames Laboratory was supported by the US Department of Energy, Basic Energy Sciences,

Division of Materials Science and Engineering, including a grant of computer time at the National Energy Research Supercomputing Centre (NERSC) in Berkeley, CA under Contract No. DE-AC02-07CH11358. Xiaojie Liu acknowledges support from China Scholarship Council (File No. 2009617104). W. C. Lu acknowledges support by the National Natural Science Foundation of China (Nos. 21043001 and 20773047).

*wangcz@ameslab.gov
†wencailu@jlu.edu.cn

[1] K. T. Chan, J. B. Neaton, and M. L. Cohen, Phys. Rev. B **77**, 235430 (2008).
[2] K. Rytkönen, J. Akola, and M. Manninen, Phys. Rev. B **75**, 075401 (2007).
[3] C. Cao, M. Wu, J. Jiang, and H.-P. Cheng, Phys. Rev. B **81**, 205424 (2010).
[4] I. Zanella, S. B. Fagan, R. Mota, and A. Fazzio, J. Phys. Chem. C **112**, 9163 (2008).
[5] X. Liu, C. Z. Wang, M. Hupalo, Y. X. Yao, M. C. Tringides, W. C. Lu, and K. M. Ho, Phys. Rev. B **82**, 245408 (2010).
[6] M. Hupalo, X. Liu, C. Z. Wang, W. C. Lu, Y. X. Yao, K. M. Ho, and M. C. Tringides, Adv. Mater. **23**, 2082 (2011).
[7] X. Liu, C. Z. Wang, Y. X. Yao, W. C. Lu, M. Hupalo, M. C. Tringides, and K. M. Ho, Phys. Rev. B **83**, 235411 (2011).
[8] M. Hupalo, S. Binz, and M. C. Tringides, J. Phys.: Condens. Matter **23**, 045005 (2011).
[9] J. Renard, M. B. Lundeberg, J. A. Folk, and Y. Pennec, Phys. Rev. Lett. **106**, 156101 (2011).
[10] M. Hupalo, E. H. Conrad, and M. C. Tringides, Phys. Rev. B **80**, 041401(R) (2009).
[11] A. T. N'Diaye, T. Gerber, C. Busse, J. Myslivecek, J. Coraux, and T. Michely, New J. Phys. **11**, 103045 (2009) and references therein.
[12] A. K. Geim, Science **324**, 1530 (2009).
[13] J. W. Evans, P. A. Thiel, and M. C. Bartelt, Surf. Sci. Reports **61**, 1 (2006).
[14] J. P. Perdew, K. Burke, and M. Ernzerhof, Phys. Rev. Lett. **77**, 3865 (1996).
[15] G. Kresse and J. Hafner, Phys. Rev. B **47**, 558 (1993).
[16] G. Kresse and J. Furthmüller, Phys. Rev. B **54**, 11169 (1996); Comput. Mater. Sci. **6**, 15 (1996).
[17] G. Makov and M. C. Payne, Phys. Rev. B **51**, 4014 (1995).
[18] J. Neugebauer and M. Scheffler, Phys. Rev. B **46**, 16067 (1992).
[19] P. E. Blöchl, Phys. Rev. B **50**, 17953 (1994).
[20] G. Kresse and D. Joubert, Phys. Rev. B **59**, 1758 (1999).
[21] W. Kohn and K. H. Lau, Solid State Comm. **18**, 553 (1976).
[22] A. V. Shytov, D. A. Abanin, and L. S. Levitov, Phys. Rev. Lett. **103**, 016806 (2009).
[23] C. Bena, Phys. Rev. Lett. **100**, 076601 (2008).
[24] A. Bacsi and A. Virosztek, Phys. Rev. B **82**, 193405 (2010).
[25] V. V. Cheianov, O. Syljuåsen, B. L. Altshuler, and V. I. Falko, Phys. Rev. B **80**, 233409 (2009).
[26] S. Saremi, Phys. Rev. B **76**, 184430 (2007).
[27] V. V. Cheianov and V. I. Falko, Phys. Rev. Lett. **97**, 226801 (2006).